Journal of Cellular and Molecular Medicine
A JOURNAL OF TRANSLATIONAL MEDICINE

J. Cell. Mol. Med. Vol 15, No 12, 2011 pp. 2697-2705

Calcitonin receptor-mediated CFTR activation in human intestinal epithelial cells

Hongguang Liu [a], Amika Singla [b], Mei Ao [b], Ravinder K. Gill [a], Jayashree Venkatasubramanian [b], Mrinalini C. Rao [b], Waddah A. Alrefai [a, c, *, #], Pradeep K. Dudeja [a, c, #]

[a] *Section of Digestive Diseases and Nutrition, Department of Medicine, University of Illinois at Chicago, Chicago, IL, USA*
[b] *Department of Physiology and Biophysics, University of Illinois at Chicago, Chicago, IL, USA*
[c] *Jesse Brown VA Medical Center, Chicago, IL, USA*

Received: August 12, 2010; Accepted: January 12, 2011

Abstract

High levels of calcitonin (CT) observed in medullary thyroid carcinoma and other CT-secreting tumours cause severe diarrhoea. Previous studies have suggested that CT induces active chloride secretion. However, the involvement of CT receptor (CTR) and the molecular mechanisms underlying the modulation of intestinal electrolyte secreting intestinal epithelial cells have not been investigated. Therefore, current studies were undertaken to investigate the direct effects of CT on ion transport in intestinal epithelial cells. Real time quantitative RT-PCR and Western blot analysis demonstrated the expression of CTR in intestinal epithelial T84 cells. Exposure of T84 cells to CT from the basolateral but not from apical side significantly increased short circuit current (I_{SC}) in a dose-dependent manner that was blocked by 1 μM of CTR antagonist, CT8–32. CT-induced I_{SC} was blocked by replacing chloride in the bath solutions with equimolar gluconate and was significantly inhibited by the specific cystic fibrosis transmembrane conductance regulator (CFTR) inhibitor, $CFTR_{127inh.}$ Further, biotinylation studies showed that CT increased CFTR levels on the apical membrane. The presence of either the Ca^{2+} chelator, bis(2-aminophenoxy)ethane tetraacetic acid-acetoxymethyl (BAPTA-AM) ester or the protein kinase A (PKA) inhibitor, H89, significantly inhibited I_{SC} induced by CT (~32–58% reduction). Response to CT was retained after permeabilization of the basolateral or the apical membranes of T84 cells with nystatin. In conclusion, the activation of CTR by CT induced chloride secretion across T84 monolayers *via* CFTR channel and the involvement of PKA- and Ca^{2+}-dependent signalling pathways. These data elucidate the molecular mechanisms underlying CT-induced diarrhoea.

Keywords: calcitonin • calcitonin receptor • chloride secretion • CFTR • diarrhoea

Introduction

Calcitonin (CT) is a 32-amino acid peptide secreted from the parafollicular cells (C-cells) of the thyroid gland and belongs to a family of peptides including CT gene-related peptide, amylin, adrenomedullin, intermedin and CT receptor (CTR)-stimulating peptide [1–4]. CT is a hypocalcaemic hormone that induces Ca^{2+} deposition in bones and stimulates calcium excretion into urine [5–7]. Clinically, CT has been used for treatment of osteoporosis, Paget's disease and hypercalcemia. CT functions by binding to its receptor, CTR, which is a class II G-protein-coupled receptor predominantly expressed in osteoclasts. CTR in osteoclasts has been previously shown to be coupled to $G\alpha$ and $G\alpha_q$ proteins that links the receptor to both adenylate cyclase–cAMP–protein kinase A (PKA) and Ca^{2+}-protein kinase C (PKC)-dependent pathways [8].

High levels of CT lead to diarrhoea. For example, diarrhoea has been reported to occur in 28–39% of patients with medullary thyroid carcinoma (MTC) associated with elevated levels of CT [9–11]. The diarrhoea in patients with MTC is usually severe, watery and lacks specific treatment and therefore, the mortality is high. Diarrhoea is also observed in other cases such as infusion of CT for hypercalcemia, CT-secreting pancreatic micro-tumours and small cell lung tumours [12–16]. Previous perfusion studies have shown that CT infusion in healthy humans and rabbits inhibited active sodium absorption and induced active chloride secretion [17, 18]. However, the detailed molecular mechanisms of CT-induced chloride secretion in intestinal epithelial cells are poorly understood.

[#]These co-senior authors contributed equally.
*Correspondence to: Waddah A. ALREFAI, M.D.,
Assistant Professor, University of Illinois at Chicago,
Jesse Brown VA Medical Center, Medical Research Service (600/151),
820 South Damen Avenue, Chicago, IL 60612, USA.
Tel.: (312) 569-7429
Fax: (312) 569-8114
E-mail: walrefai@uic.edu

doi: 10.1111/j.1582-4934.2011.01264.x

Intestinal chloride secretion plays an important role in body fluid homeostasis and diarrhoea. Several transport processes present on the basolateral and the apical membranes of intestinal cells are involved in driving chloride secretion into the intestinal epithelial lumen. The main chloride channel expressed in small intestine and colon is the cystic fibrosis transmembrane conductance regulator (CFTR). CFTR is expressed in many epithelial tissues, where it has been found to have multiple putative functions, the major one being that of a chloride channel. Activation of CFTR as a Cl^- channel requires cyclic AMP, PKA and ATP [19]. Mutations in the gene encoding CFTR leading to a decrease in chloride channel function, is the primary defect in cystic fibrosis, a disease that affects approximately 30,000 patients in the United States alone [20]. On the other hand, activation of CFTR by cholera toxin leads to a massive secretory diarrhoea and life-threatening dehydration [21]. Whether the activation of CTR by CT also stimulates chloride secretion *via* CFTR is not known.

Therefore, current studies were undertaken to investigate the expression of CTR in intestinal epithelial cells and to examine the effect of CT on electrolyte secretion in colonic T84 cell line. Our data showed that CT induced chloride secretion *via* CFTR in a Ca^{2+}- and cAMP-dependent manner. Our current studies provide novel insights into the molecular basis of CT-induced chloride secretion that may unravel potential targets for better therapy of diarrhoea associated with high levels of CT.

Materials and methods

Cell culture

Experiments were performed with the human intestinal T84 cell lines as previously described [22]. DMEM/F12 with 6% calf serum was used for T84 cells. For simultaneous measurements of [Ca^{2+}] and increased short circuit current (I_{SC}), cells were seeded onto Snapwell membranes (Costar, Corning, NY, USA) with 0.4 μm pore diameter (culture area 0.1 cm^2). Cells reached confluency after 7 to 8 days, with a resistance greater than 500 - Ω- cm^2, and then mounted in Ussing chambers (Physiologic Instruments, San Diego, CA, USA) for electrical measurements.

Real time quantitative RT-PCR analysis

RNA was extracted from T84 cells using Qiagen RNeasy kits (Qiagen, Valencia, CA, USA). Equal amounts of RNA from T84 cells were reverse transcribed and amplified in one-step reaction for β-actin and CTR by using Brilliant SYBR Green quantitative RT-PCR (QRT-PCR) Master Mix kit (Stratagene, Santa Clara, CA, USA). Real-time QRT-PCR was performed by using Mx3000P (Stratagene). Human CTR was amplified with gene-specific primers (sense primer: 5′-GCAGGAAGATGTATGCTTTGA-3′; antisense primer: 5′-CTTTACAACAGCTAGGTCCTG-3′) [23]. Human β-actin was amplified as an internal control by using gene-specific primers (sense primer: 5′-CATGTTTGAGACCTTCAACAC-3′; antisense primer: 5′-CCAGGAAGGAAGGCTGGAA-3′) [24].

Immunoblotting

For immunoblotting studies, briefly, cell lysates were prepared from T84 cells using radio immunoprecipitation assay (RIPA) buffer. A total of 100 μg protein from each of the T84 cells lysates was solubilized in Laemmli sample buffer (2% SDS, 100 mM dithiothreitol, 60 mM Tris, pH 6.8, 0.01% bromophenol blue) and was separated on 8% Tris/glycine SDS-PAGE. For CFTR, 75 μg protein from T84 cell lysate was used. The blot was then probed with primary rabbit anti-CTR antibodies (1:500, Abcam, Cambridge, MA, USA) or rabbit anti-CTR antibody (1:1000) from SantaCruz (Santa Cruz, CA, USA) or rabbit anti-actin antibody (1:5000) from Sigma (Saint Louis, MO, USA) for loading control. Goat anti-rabbit antibody (1:2000, SantaCruz) was used as secondary antibody. The bands were visualized by enhanced chemiluminescence according to the manufacturer's instructions (Amersham, Piscataway, NJ, USA).

Measurement of intracellular Ca^{2+} and cAMP levels in T84 cells

Fluo calcium indicator, Fluo-4,AM (Invitrogen, Carlsbad, CA, USA) was used for measuring intracellular [Ca^{2+}] changes after CT treatment according to company's suggested protocol. Briefly, transwell cultured T84 cells were incubated with Fluo-4,AM (5 μM) in cell culture incubator for 45 min. After washing with 1× phosphate-buffered saline (PBS), cells were incubated in 1× PBS for 30 min. to allow complete de-esterification of intracellular AM esters. The cells were then mounted on a Carl Zeiss LSM 510 laser (Carl Zeiss, Jena, Germany) scanning confocal microscope for live calcium imaging. Beam of 488 from a UV laser was used for excitation. CT was added to basolateral side at a concentration of 10 nM. Images were captured every 5 sec. for 5 min. Intracellular cAMP levels were determined using the Amersham Direct Biotrak EIA kit. On the day of assay, cells were harvested and assayed according to company's suggested protocol. Each assay point was performed at least in triplicate.

Measurements of short-circuit current

Agonist-induced anion secretion was measured in T84 monolayer as described [25, 26]. Briefly, cells grown on a Snapwell membrane were incubated with bicarbonate-buffered Krebs-Henseleit. The bicarbonate-buffered Krebs-Henseleit solution contained (in mM or mmoles/l) NaCl, 117; $NaHCO_3$, 25; KCl, 4.7; $MgSO_4$, 1.2; KH_2PO_4, 1.2; $CaCl_2$, 2.5 and D-glucose, 11, pH 7.4, when bubbled with 5% CO_2, 95% O_2. Cl^--free solution was prepared by isosmotically replacing NaCl and KCl with sodium gluconate and potassium gluconate, respectively; $CaCl_2$ was replaced with 11 mM calcium gluconate to counteract the chelating effect of gluconate anion. The potential difference was clamped to 0 mV, and I_{SC} was simultaneously measured using a voltage-clamp amplifier. Both signals were digitized and recorded. For antagonist experiments, cells were pre-incubated with the antagonist 45 min. before CT was added.

I_{SC} in nystatin-permeabilized T84 monolayers

T84 cell monolayers were mounted in the Ussing chamber and bathed in normal Krebs-Henseleit solution while the I_{SC} was measured as described above. Apical membrane Cl^- currents, defined as $I_{(ap)}$, were measured in

cells permeabilized basolaterally with 300 μg/ml nystatin in the presence of asymmetrical buffers that imposed an apical to basolateral Cl^- gradient. Basolateral NaCl was replaced by equimolar sodium gluconate. Nystatin was added to the basolateral membrane 30 min. before the addition of drugs. Under these asymmetrical conditions, activation of the apical membrane Cl^- conductance would cause a rapid downward current deflection. Basolateral membrane K^+ currents, defined as $I_{(bl)}$, were measured in cells permeabilized apically with 300 μg/ml nystatin for 30 min. in the presence of asymmetrical buffers that imposed an apical-to-basolateral K^+ gradient. The apical NaCl was replaced by equimolar K-gluconate, whereas basolateral NaCl was substituted with equimolar sodium gluconate. In all gluconate-containing solutions, $CaCl_2$ was increased to 11 mM to compensate for the Ca^{2+} chelating effect of the gluconate anion [27].

Cell surface biotinylation

Cell surface biotinylation studies were performed in T84 monolayers utilizing Sulfo-NH-SS-Biotin (1.5 mg/ml; Pierce, Rockford, IL, USA) in borate buffer (in mM: 154 NaCl, 7.2 KCl, 1.8 $CaCl_2$, 10 $H3BO_3$, pH 9.0) as described previously [28]. Labelling was allowed to proceed at 4°C to prevent endocytosis and internalization of antigens for 60 min. The biotinylated antigens were immunoprecipitated utilizing streptavidin agarose beads, and the biotinylated proteins were released by boiling in Laemmli buffer containing 100 mM dithiothreitol. Proteins were subjected to SDS-PAGE and transferred to nitrocellulose membranes for immunoblotting.

Statistical analysis

In all stances, data shown are the mean ± S.E. of three to six independent experiments. Difference between control *versus* treated was analysed using t-test and ANOVA. Differences were considered significant at $P < 0.05$.

Results

Calcitonin receptor is expressed in intestinal epithelial cells

First set of studies were undertaken to determine the expression of CTR in human intestinal epithelial cells. As shown in Figure 1A, real-time PCR analysis demonstrated the expression of CTR mRNA in human colonic T84 cell line. Western blot analysis utilizing CTR-specific antibodies also showed the presence of a ~56 kD protein band representing CTR protein (Fig. 1B). These results indicate that T84 cell line represents suitable *in vitro* cellular model for investigating the effects of CT on intestinal electrolyte transport.

Calcitonin induces short circuit current in T84 cells

Human colonic T84 cells are widely used as an *in vitro* model to study the secretory processes across colonic epithelial cells by the measurement of I_{SC} [29, 30]. Therefore, to examine the effect of CT

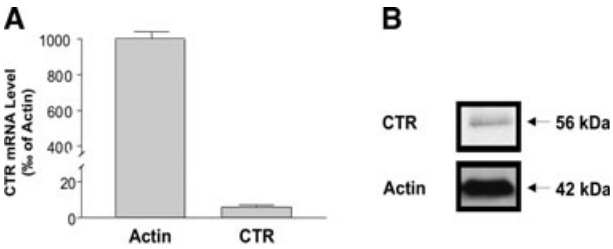

Fig. 1 CTR is expressed in intestinal epithelial cells. Total RNA from T84 cells was extracted and used for real-time QRT-PCR. (**A**) Values of mRNA levels for CTR in T84 cells were calculated based on β-actin mRNA level. Results represent mean ± S.E.M. of three independent experiments performed in triplicate. (**B**) Western Blots showed CTR protein level in T84 cells compared with β-actin.

on I_{SC}, we utilized T84 monolayers mounted in Ussing chambers. Exposure of cells to 10 nM CT added to the basolateral compartment caused a sharp increase in I_{SC} (Fig. 2C). The addition of CT from the apical side had no effect suggesting that CTR is expressed on the basolateral membrane of T84 cells. The increase in I_{SC} began within 20 sec. of addition of CT, peaked at 5–10 min. and started to return to baseline slowly by 45–60 min. When compared to the actions of carbachol (CCH, 100 μM) (Fig. 2A) or Forskolin (FSK (10 μM) (Fig. 2B), CT-induced I_{SC} was much longer in duration than CCH, but shorter than FSK; it was slower than CCH but more rapid than FSK to reach its peak. CT-induced I_{SC} in the T84 monolayer was concentration dependent, *i.e.* 10 nM produced higher effects than 1 nM, and interestingly, 100 nM had less effect than 10 nM (Fig. 2D). Pre-incubation (30 min.) of the T84 monolayer with increasing concentrations of CTR-specific antagonist, $CT_{8–32}$ resulted in a dose-dependent blockage of CT-induced I_{SC}, with 1 μM of $CT_{8–32}$ almost completely abolishing CT- (10 nM) induced I_{SC} (3.1 ± 1.1% of control) (Fig. 2E). Inhibition only occurred when $CT_{8–32}$ was added to the basolateral not the apical side, further indicating a functional basolateral distribution of CTR in this cell line.

CT-induced I_{SC} in T84 cell monolayer is Cl^- dependent

To test whether CT-induced I_{SC} in T84 cells results from Cl^- secretion, T84 monolayer was mounted in Ussing chambers and Cl^- was replaced with equimolar gluconate in the bathing solutions. As shown in Figure 3A, Cl^--free conditions produced a significant reduction of I_{SC} (12.5 ± 6.0% of Cl^- containing medium, $P < 0.001$) at 1 min., and was abolished (5.4 ± 1.3% of Cl^- containing medium, $P < 0.001$) at 5 min. after basolateral application of CT. To further determine the nature of the CT-induced I_{SC}, we tested the effects of inhibitors of transport pathways involved in chloride secretion. As depicted in Figure 3B and C, the addition of 100 μM bumetanide, a specific blocker of sodium, potassium, chloride co-transporter (NKCC)1, to the basolateral side caused a significant decrease (12.5 ± 6.0%, compared to 80 ± 7.6% of peak I_{SC} with

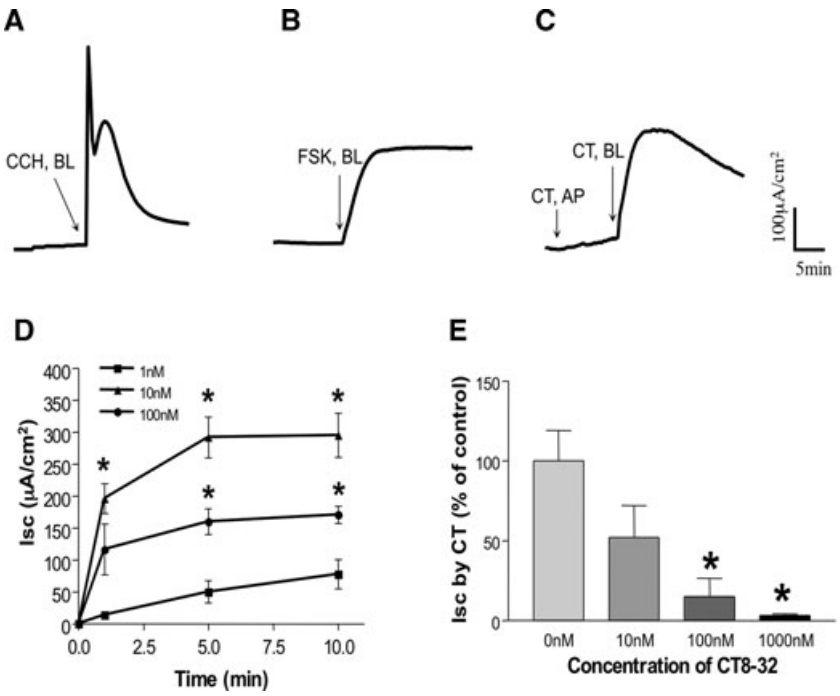

Fig. 2 CT-induced I_{SC} in T84 monolayers. A representative tracing is shown here: (**A**) CCH (100 μM), (**B**) FSK (10 μM) when added from the basolateral side of the T84 cell monolayer after the baseline was established. In (**C**), CT (10 nM) was initially added from the apical compartment (AP), then at the basolateral side (BL) of the T84 monolayer. (**D**) Dose–response. CT was added from the basolateral side of the T84 cell monolayer after the baseline was established at different concentrations: 1, 10 and 100 nM. Values represent the mean ± S.E. of three independent determinations. $^*P < 0.001$ compared to cell treated with 1 nM. (**E**) T84 cell monolayer was pre-incubated with CT antagonist, CT8–32 at different concentrations for 20 min. from the basolateral side, then CT (10 nM) was added also from the basolateral side for 10 min. Values shown here are the percentage of control (*i.e.* without CT8–32) and represent the mean ± S.E. of three independent determinations. $^*P < 0.001$.

vehicle alone). Barium chloride (5 mM), a general inhibitor for K^+ channels, also resulted in significant decrease in I_{SC} induced by CT (13.3 ± 3.3%, compared to 80 ± 7.6% of peak I_{SC} with vehicle alone) when added from the basolateral side (Fig. 3D and F). Furthermore, the addition of 10 μM of $CFTR_{inh}172$ (a specific inhibitor for CFTR), significantly reduced CT-induced I_{SC} when added to the apical side as shown in Figure 3E and F (I_{SC} induced by CT decreased to 11.7 ± 4.4%, compared to 80 ± 7.6% of peak I_{SC} with vehicle alone). These data suggested that the CT-induced I_{SC} in T84 cells is contributed by K^+ channels, CFTR and NKCC.

PKA- and Ca^{2+}-dependent pathways are involved in CT-induced Cl^- secretion

Activation of CTR in osteoclasts has been previously shown to stimulate both adenylate cyclase/cAMP/PKA and Ca^{2+}/PKC intracellular signalling pathways [8]. In order to determine if CT-induced chloride secretion in T84 cells involves Ca^{2+}-dependent pathways, we examined if there were changes in intracellular Ca^{2+} in these cells in response to CT. The results depicted in Figure 4A showed that intracellular Ca^{2+} signal increased almost immediately after addition of 10 nM of CT to the basolateral side, and kept elevated for more than 5 min. We also measured intracellular cAMP levels in T84 cells to determine if CT-induced chloride secretion involves the cAMP signalling mechanism. Intracellular cAMP levels increased from baseline 93 ± 12 fmol/μg protein to 9000 ± 346 fmol/μg protein after 20 min. incubation with 10 nM CT (Fig. 4B). The CT effect was blocked (9000 ± 346 fmol/μg protein *versus* 157 ± 19 fmol//μg protein) by co-incubation with 1000 nM of the CT antagonist CT8–32, while CT8–32 alone had no effect on intracellular cAMP level (93 ± 12 fmol/well *versus* 125 ± 25 fmol/μg protein). FSK (10 μM), used as a positive control, similarly increased cAMP level (17105 ± 2421 fmol/μg protein).

We next examined the effect of H-89, a PKA inhibitor, and RpcAMP, a cAMP antagonist to further confirm the involvement of the PKA-cAMP pathway in CT-induced chloride secretion. As shown in Figure 4C, pre-treatment of T84 cells with the H-89 (10 μM) or RpcAMP (25 μM) for 45 min., reduced CT-mediated I_{SC} to 45.8 ± 8.2% and 68.5 ± 3.9% of control, respectively.

In order to assess the role of Ca^{2+} or PKC pathways in CT-induced chloride secretion in T84 cells, BAPTA-AM (Ca^{2+} chelator) and bisindolylmaleimide (BIM) (general PKC inhibitor) [31] were used. Pre-incubation of T84 cells with 20 μM BAPTA-AM for 45 min. resulted in 42.4 ± 13.2% of CT-induced I_{SC}, whereas BIM (5 μM) had no effect (Fig. 4C). These results indicate that cAMP and Ca^{2+}-dependent but not PKC-dependent pathways are involved in the effects of CT. Interestingly, pre-incubation with both 20 μM BAPTA-AM and 10 μM H-89 produced an additive effects (decreased to 25.2 ± 2.3% of control, Fig. 4C) suggesting each of the cAMP and Ca^{2+}-pathways has separate effects on CT-induced I_{SC}.

CT stimulates I_{SC} across the apical and basolateral membranes of intestinal epithelial cells

To further delineate the involvement of apical conductance and/or basolateral conductance in the T84 monolayer, the pore-forming

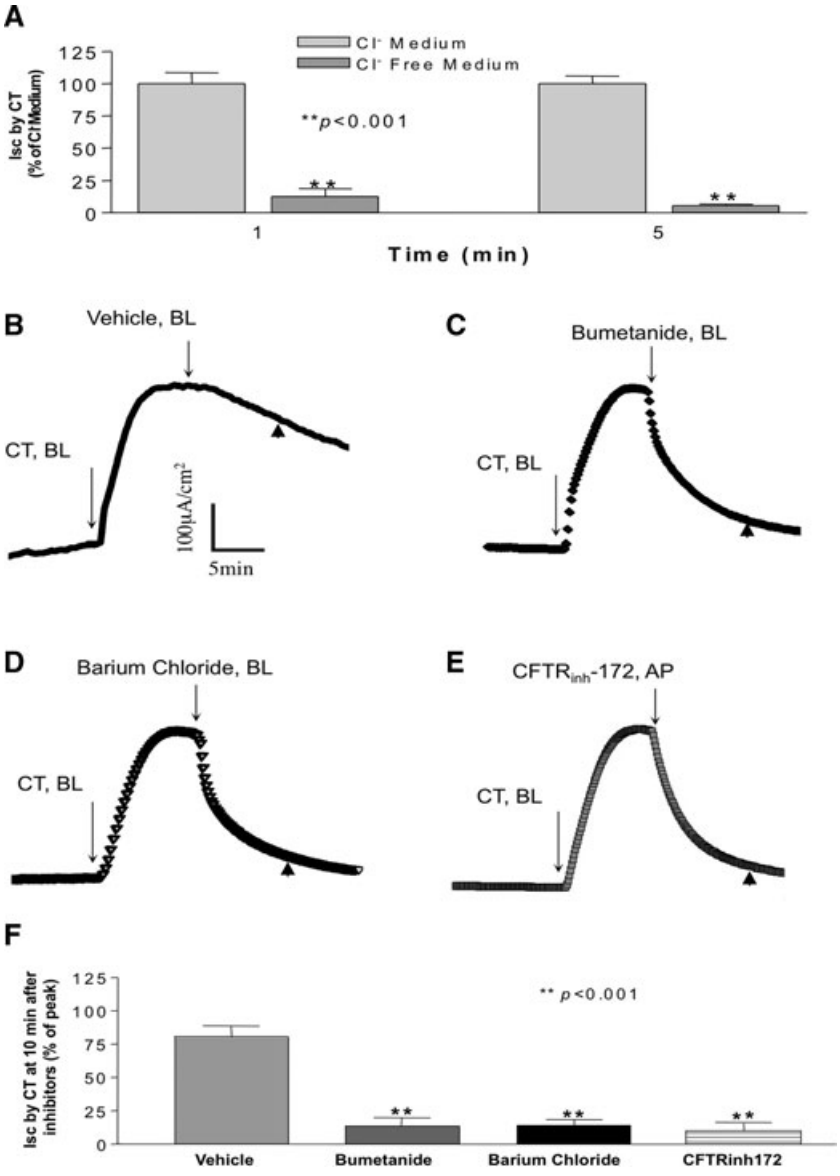

Fig. 3 CT-induced I_{SC} is chloride dependent. (**A**) CT (10 nM) was added from the basolateral side in regular Cl^- containing Krebs-Henseleit medium and Cl^- free Krebs-Henseleit medium where Cl^- was replaced with equimolar gluconate. Data shown here are 1 and 5 min. after adding CT, calculated as percentage of Cl^- containing Krebs-Henseleit medium. For studying the effects of different inhibitors, CT (10 nM) was added from the basolateral side after establishment of the baseline. Ten minutes later, inhibitors: (**B**) control = vehicle, (**C**) Bumetanide (100 μM), (**D**) barium chloride (5 mM) were added from the basolateral side, and (**E**) $CFTR_{inh}$-172 (10 μM) was added from the apical compartment of the T84 monolayer. One representative tracing of each is shown here. (**F**) Data shown here are the values of I_{SC} 10 min. after addition of different inhibitors (control = vehicle, Bumetanide, barium chloride, $CFTR_{inh}$-172) (arrowhead in **B**, **C**, **D** and **E**), calculated as percentage of control. Results represent mean ± S.E.M. of three or more independent experiments in all above figures. $^{**}P < 0.001$.

antibiotic nystatin was used to selectively permeabilize either cellular membrane [25]. The appropriate transepithelial ion gradients were also established to measure the apical $I_{(ap)}$ and basolateral $I_{(bl)}$ currents. CT was added to basolateral side in both conditions. $I_{(ap)}$ was measured after nystatin permeabilization of the basolateral membrane. The CT-induced $I_{(ap)}$ was significantly blocked (28.4 ± 8.7%, Fig. 5A and C) by H89 (10 μM, 45 min. pre-incubation), while BAPTA-AM (30 μM, 45 min. pre-incubation) alone had no effect in this setting (86.1 ± 13.5%, Fig. 5C). This current was also sensitive to $CFTR_{inh172}$, which represented a CFTR current (Fig. 5A). After nystatin permeabilization of the apical membrane, application of CT generated a small I_{bl}, which was significantly blocked by 45 min. pre-incubation of 20 μM of BAPTA-AM and 10 μM of H89; however, H89 had much less effect (21.2 ± 7.3% of control for BAPTA-AM and 50.0 ± 11.2% of control for H89, $P < 0.01$, Fig. 5B and D). This current was not found to be sensitive to NKCC inhibitor, bumetanide, but sensitive to K^+ channel blocker, barium chloride, which represented a K^+ channel current (Fig. 5B). These results suggest that CT evokes both I_{SC} across the apical membrane *via* CFTR, and I_{SC} current across the basolateral membrane *via* K^+ channels. These findings also suggest that cAMP signalling component of CT-induced I_{SC} involves both apical and basolateral processes, while Ca^{2+} component mostly involves basolateral process induced by CT.

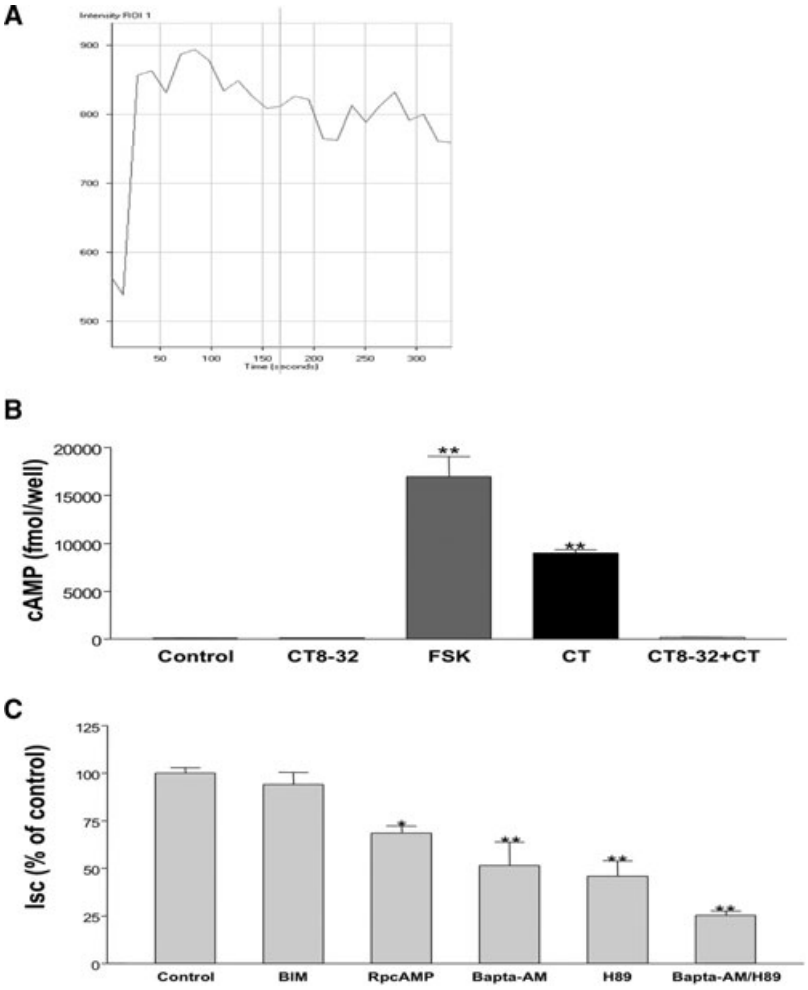

Fig. 4 CT-induced Cl^- secretion involves Ca^{2+}- and PKA- dependent pathways. (**A**) Live calcium imaging study was used to detect intracellular Ca^{2+} signal after adding 10 nM of CT to the basolateral side according to manufacturer's protocol (*y*-axis represent the intensity of the signal indicating the level of intracellular Ca^{2+}) (**B**) Intracellular cAMP was measured according to manufacturer's protocol 10 min. after basolateral addition of control (vehicle), CT8–32 (1000 nM), FSK (10 μM), CT (10 nM) or CT (10 nM) with 30 min. of pre-incubation of CT8–32 (1000 nM). (**C**) CT (10 nM) was added from basolateral side 45 min. after incubation with control = vehicle, BIM (5 μM), RpcAMP (25 μM), BAPTA-AM (20 μM), H89 (10 μM) or BAPTA-AM (20 μM) combined with H89 (10 μM) from both apical and basolateral sides. Data were calculated as percentage of control obtained from 10 min. after adding CT. Results represent mean ± S.E.M. of five or more independent experiments in all above figures. $^*P < 0.01$, $^{**}P < 0.001$.

CT increased CFTR levels on the apical membrane

A mechanism of activation of CFTR is an increase in its trafficking from the intracellular compartments to the membrane. Aberrations in trafficking are among the causes underlying the manifestation of the disease in CF patients. To examine whether CT increases I_{SC} *via* altering the membrane levels of CFTR, cell surface biotinylation studies were performed. Results showed that CT treatment (20 min.) of T84 cells significantly increased the surface level of CFTR compared to control (Fig. 6).

Discussion

Previous studies have shown that CT stimulates active Cl^- secretion in adult rat ileum *in vitro* [32], rabbit *in vivo* [17, 33] and healthy humans *in vivo* [18]. The current studies provide more in depth understanding of the mechanisms of intestinal chloride secretion induced by CT. The major findings of current studies are: (*i*) CTR is expressed in human colonic epithelial cells; (*ii*) direct activation of CTR by CT in intestinal epithelial cells; (*iii*) CT-induced Cl^- secretion involves both Ca^{2+}- and cAMP-dependent pathways; (*iv*) CT-induced Cl^- secretion occurs *via* CFTR chloride channel.

Earlier studies demonstrated the expression of CTR in several cell types including cells in the central nervous system, renal epithelial cells, breast, prostate cells and abundantly in mature osteoclasts [34]. CT was shown to inhibit sodium, hydrogen exchanger (NHE) activity and the Na, K-ATPase in the kidney cell line LLC-PK1 [29]. CT was also found to inhibit proton extrusion in resorbing rat osteoclasts *via* PKA [30]. Although, previous studies showed that CT-induced chloride secretion was observed in human beings and rabbits, no information was available regarding the mechanisms of CT-induced chloride secretion, including CTR expression and its direct activation in intestinal epithelial cells. Our findings provided novel evidence showing the expression of CTR in colonic T84 cell line both at the mRNA and protein levels. These

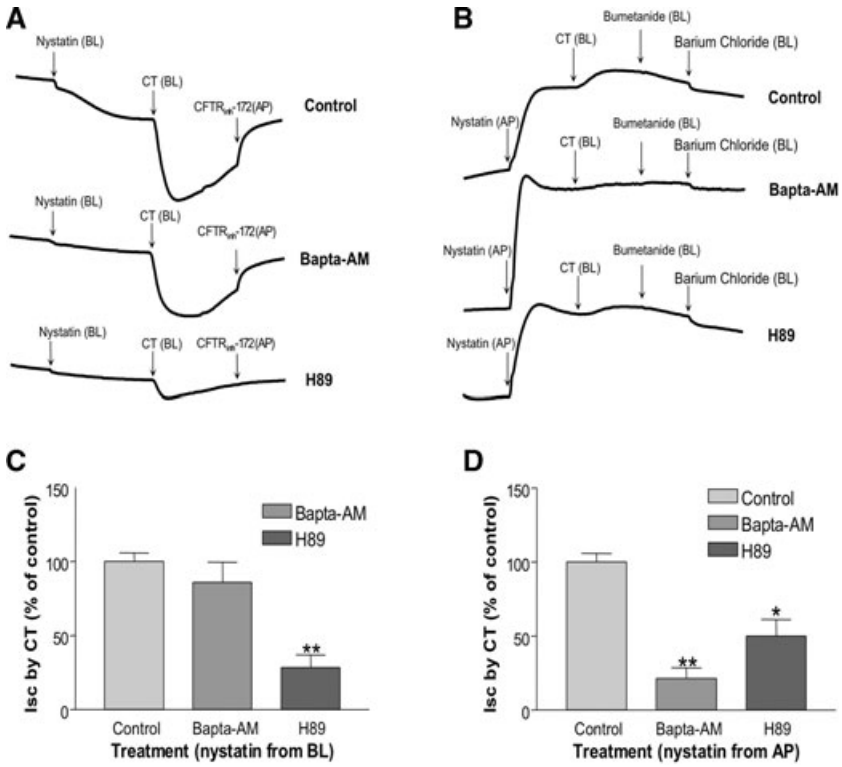

Fig. 5 CT-induced I_{SC} involved Ca^{2+}- and PKA-dependent pathways in Nystatin-permeabilized preparations. (**A**) T84 cell monolayer was pre-incubated either with vehicle (control), BAPTA-AM (20 μM) or H89 (10 μM) from both the basolateral and apical sides for 45 min. Then the regular basolateral Krebs-Henseleit solution was replaced with a lower [Cl^-] Krebs-Henseleit medium, so that a chloride gradient was maintained from the apical to basolateral. After stabilizing the baseline, Nystatin (300 μg/ml) was added from the basolateral side. CT (10 nM) was then added from the basolateral side after the baseline was stabilized. $CFTR_{inh}$-172 was added from the apical compartment after the peak of CT-induced I_{SC}. (**B**) T84 cell monolayer was pre-incubated either with control = vehicle, BAPTA-AM (20 μM) or H89 (10 μM) from both the basolateral and apical sides for 45 min. Then the regular basolateral Krebs-Henseleit solution was replaced with a lower [K^+] Krebs-Henseleit medium, so that a [K^+] gradient was achieved from the apical to basolateral. After stabilizing the baseline, Nystatin (300 μg/ml) was added from the apical compartment. CT (10 nM) was then added from the basolateral side after the baseline was stabilized. Bumetanide (100 μM) and barium chloride (5 mM) were separately added from the basolateral side after the peak of CT-induced I_{SC}. (**C**) Data shown here are the peak I_{SC} induced by CT from different pre-treatments: control = vehicle, BAPTA-AM and H89 in (**A**), which were calculated as percentage of control. (**D**) Data shown here are the peak I_{SC} induced by CT from different pre-treatments: control (vehicle), BAPTA-AM and H89 in (**B**), which were calculated as percentage of control. Results represent mean ± S.E.M. of three or more independent experiments in all above figures. * $P < 0.01$, ** $P < 0.001$.

findings provided a compelling evidence for the suitability of these intestinal cell lines to be used as an *in vitro* cellular model to investigate the molecular mechanisms underlying electrolyte transport alterations by CT.

In the T84 cell model, when CT was added to the basolateral side of T84 monolayer, an I_{SC} was generated almost immediately, which was blocked by CTR-specific antagonist CT8–32 in a dose-dependent manner, while no current was produced when CT was added from the apical compartment. These findings indicate that this I_{SC} was induced by CTR located on the basolateral membrane of the T84 cells, which is consistent with the fact that CT is a blood borne hormone. It is interesting that CT at 10 nM concentration induced chloride secretion more than at 100 nM concentration. As 10 and 100 nM CT-induced cAMP levels to the same extent (data not shown), we believe that this observation is likely due to a receptor de-sensitization. Indeed, diarrhoea occurs in about 28–39% of patients with MTC associated with high CT. These individual differences may reflect different levels of CTR expression in the intestinal epithelial cells or may indicate individual variations in the mechanisms involved in receptor desensitization.

Further experiments confirmed that CT-induced I_{SC} in T84 monolayers was indeed due to increases in chloride secretion involving apical CFTR and basolateral NKCC and potassium channels (Figs 2 and 3). Further, biotinylation studies showed that CT increased CFTR levels on the apical membrane. Our findings also demonstrated that after activation of CTR by CT, two intracellular signalling pathways are triggered in T84 cells: cAMP- and Ca^{2+}-dependent pathways. The earlier studies in rats, rabbits and humans, measured only the total amount of electrolyte movements across of the intestinal epithelia. There are no data delineating the signalling pathways in intestinal epithelial cells. Our data showed that the direct activation of CTR by CT in T84 monolayers, significantly increased intracellular cAMP levels, which then either directly activated CFTR or stimulated basolateral membrane K^+ channel activity. The basolateral K^+ channels, promote potassium recycling across the basolateral membrane by extruding K^+ entering either *via* the NKCC cotransporter or the Na, K-ATPase pump, and thereby increasing the electrochemical gradient for Cl^- entering *via* NKCC to exit the cell *via* apical membrane chloride channels (Figs 4 and 5). Our findings also demonstrated that CT caused an immediate increase in Ca^{2+} and the BAPTA data showed that the role of Ca^{2+} in CT evoked chloride secretion was through K^+ channels on the basolateral membrane (Figs 4 and 5). Although activating distinct pathways, $Ca^{2+}$and cyclic nucleotides often modulate each other's activities and the fact that CT activates both provides some intriguing possibilities for exploring the cross-talk between

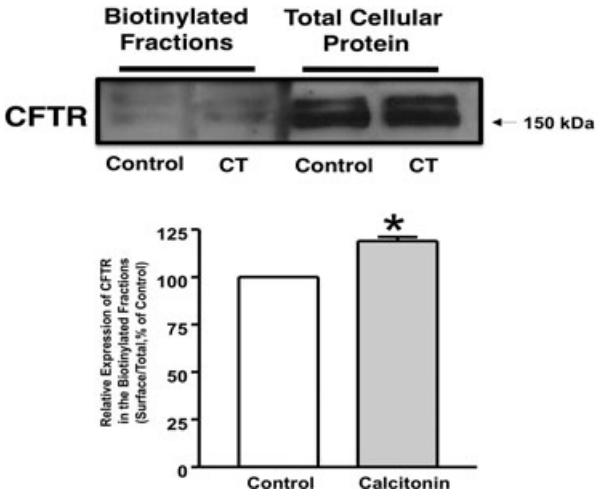

Fig. 6 CT increased CFTR level on apical membrane. T84 cells were plated in transwells. Cells were treated with CT (10 nM) or vehicle for 20 min. and then subjected to biotinylation at 4°C utilizing sulfo-NH-SS-biotin. Biotinylated proteins were extracted with streptavidin-agarose, and surface and total fractions were run on 8% SDS-PAGE. The blot was immunostained with rabbit anti-CFTR antibody. Representative blots of three separate experiments are shown. Quantification data from densitometric analysis are shown from three different experiments. Values are expressed as percentage of control and represent mean ± S.E. $*P < 0.05$.

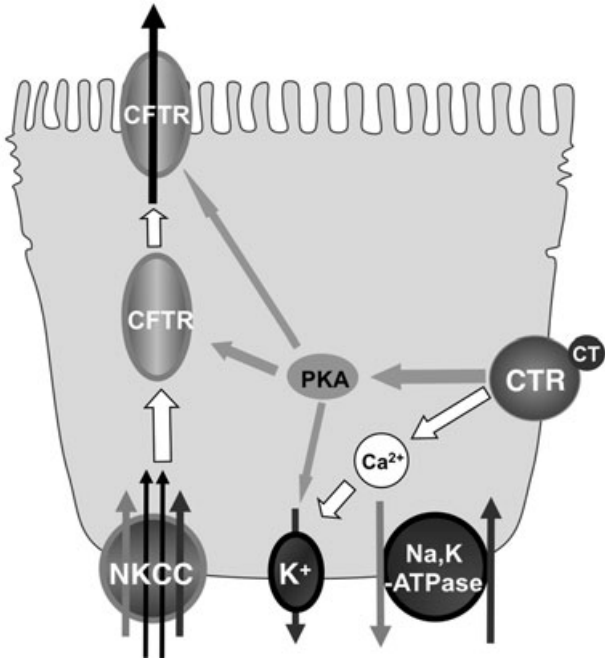

Fig. 7 Proposed cell signalling pathways of CTR mediated CFTR activation.

the two cascades. Responses to cyclic nucleotide-mediated agonists are sustained, whereas those to Ca^{2+}-mediated agonists are transient even though levels of intracellular Ca^{2+} can remain elevated after the secretory response has resolved [35]. This may explain the fact that CT-induced chloride secretion has a unique feature: quick response that could be due to activation of Ca^{2+}-dependent pathway like CCH and longer duration that may result from activation of cAMP-dependent pathway like FSK (Fig. 2**)**.

Based on our findings, we propose the following cell signalling pathways of CTR mediated CFTR activation (Fig. 7). CT binds and activates CTR located at the basolateral membrane of T84 cells, which then evokes cAMP- and Ca^{2+}-dependent pathways stimulating CFTR and secreting chloride. In cAMP-dependent pathway, cAMP not only affects CFTR directly, either by activating CFTR channels or by increasing CFTR levels on the apical membrane, but also activates K^+ channel on the basolateral membrane. In Ca^{2+}-dependent pathways, Ca^{2+} activates the K^+ channel at the basolateral side providing the driving force for chloride influx *via* NKCC.

The current findings of CTR expression in intestinal epithelial cells provide a possible target for managing CT-induced severe diarrhoea in MTC patients, especially patients with liver metastasis. Most patients have more than 12 bowel movements a day, thus the mortality is high due to dehydration. Currently, specific treatment for such a condition is not available. CT8–32, a peptide lacking the critical N-terminal 7 amino acids, showed significant blocking of the effects of CT-induced chloride secretion. Therefore, targeting at CTR may help to develop some novel therapeutic modality to treat CT-induced diarrhoea in MTC patients and other clinical situations where severe diarrhoea is developed in CT-secreting pancreatic micro-tumour, and small cell lung tumours, etc.

In summary, the current study showed for the first time the expression of CTR in intestinal epithelial cells. Our data further demonstrated that CT, a hormone that regulates calcium homeostasis, directly activates CTR and induces CFTR-mediated chloride secretion in intestinal epithelial cells *via* cAMP- and Ca^{2+}-dependent signalling pathways. Our results define the molecular mechanisms underlying CT effects on intestinal ion transport and may enhance the possibility of developing novel therapeutic approaches for the treatment CT-induced diarrhoea.

Conflict of interest

The authors confirm that there are no conflicts of interest.

Acknowledgements

These studies were supported by the Department of Veterans Affairs (P.K.D. and W.A.A.) and the NIDDK grants: DK54016 (P.K.D.), DK81858 (P.K.D.), DK71596 (W.A.A.), DK74458 (R.K.G.) and the Program Project Grant DK67887 (P.K.D. and M.C.R.) and the training grant T32DK007788 (H.L.).

References

1. **Wimalawansa SJ.** Amylin, calcitonin gene-related peptide, calcitonin, and adrenomedullin: a peptide superfamily. *Crit Rev Neurobiol*. 1997; 11: 167–239.
2. **Chang CL, Roh J, Hsu SY.** Intermedin, a novel calcitonin family peptide that exists in teleosts as well as in mammals: a comparison with other calcitonin/intermedin family peptides in vertebrates. *Peptides*. 2004; 25: 1633–42.
3. **Roh J, Chang CL, Bhalla A, *et al.*** Intermedin is a calcitonin/calcitonin gene-related peptide family peptide acting through the calcitonin receptor-like receptor/receptor activity-modifying protein receptor complexes. *J Biol Chem*. 2004; 279: 7264–74.
4. **Granholm S, Lundberg P, Lerner UH.** Calcitonin inhibits osteoclast formation in mouse haematopoetic cells independently of transcriptional regulation by receptor activator of NF-{kappa}B and c-Fms. *J Endocrinol*. 2007; 195: 415–27.
5. **Warshawsky H, Goltzman D, Rouleau MF, *et al.*** Direct *in vivo* demonstration by radioautography of specific binding sites for calcitonin in skeletal and renal tissues of the rat. *J Cell Biol*. 1980; 85: 682–94.
6. **Chambers TJ, Magnus CJ.** Calcitonin alters behaviour of isolated osteoclasts. *J Pathol*. 1982; 136: 27–39.
7. **Davey RA, Morris HA.** The effects of salmon calcitonin-induced hypocalcemia on bone metabolism in ovariectomized rats. *J Bone Miner Metab*. 2005; 23: 359–65.
8. **Purdue BW, Tilakaratne N, Sexton PM.** Molecular pharmacology of the calcitonin receptor. *Receptors Channels*. 2002; 8: 243–55.
9. **Deftos LJ, Bury AE, Habener JF, *et al.*** Immunoassay for human calcitonin. II. Clinical studies. *Metabolism*. 1971; 20: 1129–37.
10. **Melvin KE, Tashjian AH Jr, Miller HH.** Studies in familial (medullary) thyroid carcinoma. *Recent Prog Horm Res*. 1972; 28: 399–470.
11. **Rambaud JC, Jian R, Flourie B, *et al.*** Pathophysiological study of diarrhoea in a patient with medullary thyroid carcinoma. Evidence against a secretory mechanism and for the role of shortened colonic transit time. *Gut*. 1988; 29: 537–43.
12. **Kelley MJ, Snider RH, Becker KL, *et al.*** Small cell lung carcinoma cell lines express mRNA for calcitonin and alpha- and beta-calcitonin gene related peptides. *Cancer Lett*. 1994; 81: 19–25.
13. **Kelley MJ, Becker KL, Rushin JM, *et al.*** Calcitonin elevation in small cell lung cancer without ectopic production. *Am J Respir Crit Care Med*. 1994; 149: 183–90.
14. **Eskens FA, Roelofs EJ, Hermus AR, *et al.*** Pancreatic islet cell tumor producing vasoactive intestinal polypeptide and calcitonin. *Anticancer Res*. 1997; 17: 4667–70.
15. **Mullerpatan PM, Joshi SR, Shah RC, *et al.*** Calcitonin-secreting tumor of the pancreas. *Dig Surg*. 2004; 21: 321–4.
16. **Jackson C, Buchman AL.** Calcitonin-secreting VIPoma. *Dig Dis Sci*. 2005; 50: 2203–6.
17. **Gray TK, Juan D, Powell DW.** Salmon calcitonin and water and electrolyte transport in rabbit ileum. *Proc Soc Exp Biol Med*. 1975; 150: 151–4.
18. **Gray TK, Brannan P, Juan D, *et al.*** Ion transport changes during calcitonin-induced intestinal secretion in man. *Gastroenterology*. 1976; 71: 392–8.
19. **Jovov B, Ismailov, II, Berdiev BK, *et al.*** Interaction between cystic fibrosis transmembrane conductance regulator and outwardly rectified chloride channels. *J Biol Chem*. 1995; 270: 29194–200.
20. **Verkman AS, Galietta LJ.** Chloride channels as drug targets. *Nat Rev Drug Discov*. 2009; 8: 153–71.
21. **Thiagarajah JR, Verkman AS.** New drug targets for cholera therapy. *Trends Pharmacol Sci*. 2005; 26: 172–5.
22. **Hecht G, Hodges K, Gill RK, *et al.*** Differential regulation of Na+/H+ exchange isoform activities by enteropathogenic E. coli in human intestinal epithelial cells. *Am J Physiol Gastrointest Liver Physiol*. 2004; 287: G370–8.
23. **Granfar RM, Day CJ, Kim MS, *et al.*** Optimised real-time quantitative PCR assays for RANKL regulated genes. *Mol Cell Probes*. 2005; 19: 119–26.
24. **Alrefai WA, Annaba F, Sarwar Z, *et al.*** Modulation of human Niemann-Pick C1-like 1 gene expression by sterol: role of sterol regulatory element binding protein 2. *Am J Physiol Gastrointest Liver Physiol*. 2007; 292: G369–76.
25. **Yue GG, Yip TW, Huang Y, *et al.*** Cellular mechanism for potentiation of Ca2+-mediated Cl- secretion by the flavonoid baicalein in intestinal epithelia. *J Biol Chem*. 2004; 279: 39310–6.
26. **Bijvelds MJ, Bot AG, Escher JC, *et al.*** Activation of intestinal Cl- secretion by lubiprostone requires the cystic fibrosis transmembrane conductance regulator. *Gastroenterology*. 2009; 137: 976–85.
27. **Ko WH, Chan HC, Chew SB, *et al.*** Ionic mechanisms of Ca(2+)-dependent electrolyte transport across equine sweat gland epithelium. *J Physiol*. 1996; 493: 885–94.
28. **Borthakur A, Gill RK, Tyagi S, *et al.*** The probiotic Lactobacillus acidophilus stimulates chloride/hydroxyl exchange activity in human intestinal epithelial cells. *J Nutr*. 2008; 138: 1355–9.
29. **Dharmsathaphorn K, McRoberts JA, Mandel KG, *et al.*** A human colonic tumor cell line that maintains vectorial electrolyte transport. *Am J Physiol*. 1984; 246: G204–8.
30. **Chow JY, Barrett KE.** Role of protein phosphatase 2A in calcium-dependent chloride secretion by human colonic epithelial cells. *Am J Physiol Cell Physiol*. 2007; 292: C452–9.
31. **Saksena S, Dwivedi A, Gill RK, *et al.*** PKC-dependent stimulation of the human MCT1 promoter involves transcription factor AP2. *Am J Physiol Gastrointest Liver Physiol*. 2009; 296: G275–83.
32. **Walling MW, Brasitus TA, Kimberg DV.** Effects of calcitonin and substance P on the transport of Ca, Na and Cl across rat ileum *in vitro*. *Gastroenterology*. 1977; 73: 89–94.
33. **Kisloff B, Moore EW.** Effects of intravenous calcitonin on water, electrolyte, and calcium movement across *in vivo* rabbit jejunum and ileum. *Gastroenterology*. 1977; 72: 462–8.
34. **Nishikawaa T, Ishikawa H, Yamamotoa S, *et al.*** A novel calcitonin receptor gene in human osteoclasts from normal bone marrow. *FEBS Letter*. 1999; 458: 409–14.
35. **Keely SJ, Barrett KE.** p38 mitogen-activated protein kinase inhibits calcium-dependent chloride secretion in T84 colonic epithelial cells. *Am J Physiol Cell Physiol*. 2003; 284: C339–48.